PVRIG Expression is Associated With T Cell Exhaustion and Synergizes With TIGIT to Inhibit Anti-Tumor Responses

Eran Ophir[1], Maya Kotturi[2], Ofer Levy[1], Sarah Whelan[2], Sudipto Ganguly[3], Ling Leung[2], Liat Dassa[1], Zoya Alteber[1], Arthur Machlenkin[1], Drew Pardoll[3], Mark White[2], Spencer Liang*[2]

[1]Compugen Ltd, Holon Israel; [2]Compugen USA, Inc, South San Francisco CA; [3]Bloomberg Kimmel Institute for Cancer Immunotherapy, Johns Hopkins University, Baltimore, MD

compugen FROM CODE TO CURE

Poster#2028

ABSTRACT

By employing a unique computational discovery platform, we identified a novel checkpoint receptor family comprised of two inhibitory receptors in the nectin family, TIGIT and PVRIG. PVRIG and TIGIT are both expressed upon T cell activation, but display a difference in relative expression among T cell subsets and expression kinetics. PVRIG binds to PVRL2 whereas TIGIT binds to several ligands, among which we observed that PVR is the dominant functional ligand for TIGIT. The distinct expression profile of PVRIG and a unique high affinity PVRIG-PVRL2 interaction suggest that PVRIG has a unique role in regulating immunity. Using novel PVRIG$^{-/-}$ mice, we observed that genetic deficiency of PVRIG resulted in increased T cell responses and reduced tumor growth in preclinical models, demonstrating the potential of targeting this pathway in cancer. To further define a clinical niche for a PVRIG antagonist, we interrogated the expression of TIGIT/PVRIG and PD-1 axis in human tumor samples. Among the human cancers examined, PVRIG and TIGIT expression on tumor derived T cells were highest in endometrial, lung, kidney, and ovarian cancers. A co-expression analysis of PVRIG, TIGIT, and PD-1 demonstrated that PVRIG was correlated and co-expressed with both TIGIT and PD-1 and that PVRIG^{+}TIGIT^{+}PD-1^{+} cells comprised a major percentage of CD8 tumor infiltrating lymphocytes (TILs). Interestingly, PVRIG and not TIGIT expression on CD8^{+} TILs were associated with an exhausted Eomes^{hi}T-bet^{lo} phenotype. PVR, PVRL2, and PD-L1 also displayed tissue specific differences in relative expression level, with endometrial and ovarian tumors having a higher ratio of PVRL2 expression relative to PVR or PD-L1. Culture of primary human TILs with anti-PVRIG (COM701) and anti-TIGIT (COM902) antagonistic antibodies enhanced T cell function to a similar or greater magnitude compared to PD-1 blockade.

COM701 & COM902 TARGET PVRIG AND TIGIT IN THE NECTIN & NECTIN-LIKE FAMILY

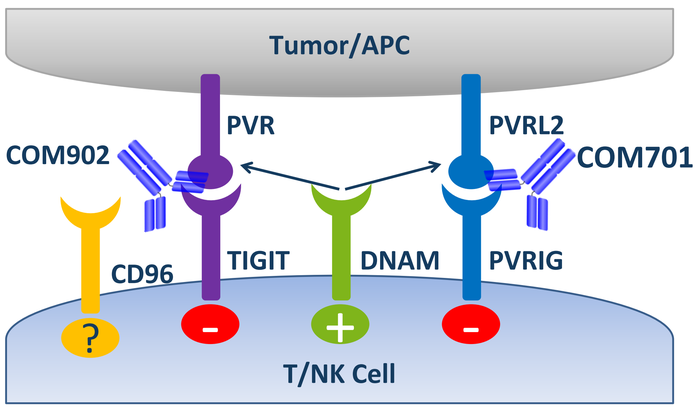

PVRIG ANTIBODY BLOCKADE OR DEFICIENCY RESULT IN REDUCED TUMOR GROWTH

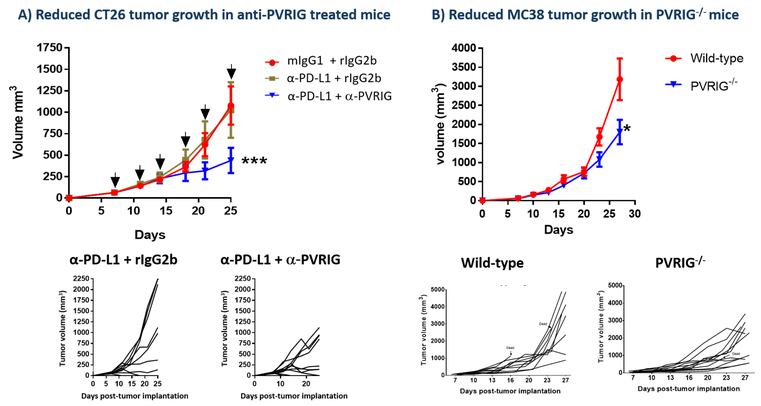

Figure 1. PVRIG antibody blockade or deficiency inhibit tumor growth. A) BALB/c mice were subcutaneously injected with 5×10^5 CT26 cells. At day 7 post inoculation mice were treated with anti-PD-L1 and/or anti-PVRIG antibodies, twice weekly for 3 weeks. Tumor volumes are shown. n=10 mice per group. Mean +/- SEM is shown. *** Indicates p-value < 0.001 (ANOVA with repeated measures) for anti-PD-L1 + Rat IgG2b compared to anti-PD-L1 + anti-PVRIG treated groups. B) C57BL/6 WT or PVRIG$^{-/-}$ mice were subcutaneously injected with 5×10^5 MC38 cells. n=10 mice per group. Mean +/- SEM is shown. *Indicates p-value < 0.05 for WT mice versus PVRIG$^{-/-}$ mice (ANOVA with repeated measures). Individual tumor growth curves are also shown. Representative data from n=2 experiments.

EXPRESSION PROFILING OF PVRIG/TIGIT AXIS IN HUMAN TUMORS

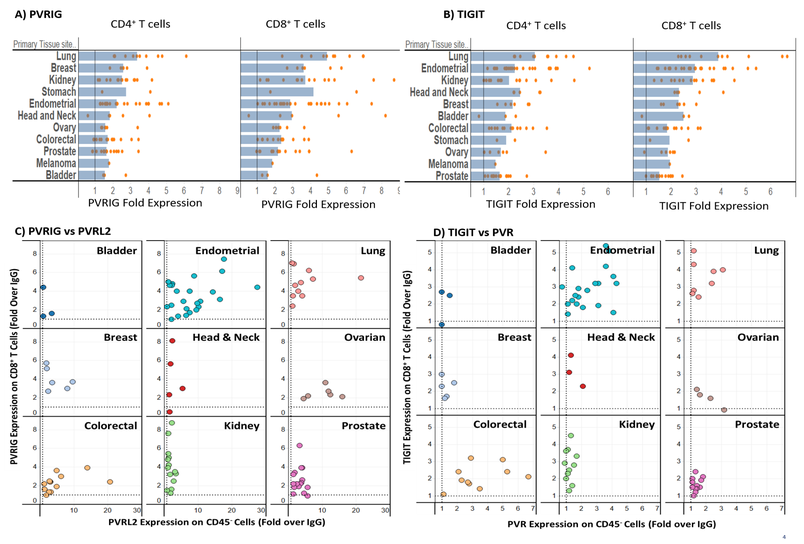

Figure 2. Lung and endometrial cancers are high for both PVRIG-PVRL2 and TIGIT-PVR pathway. (A, B) PVRIG and TIGIT expression were analyzed on CD4^{+} and CD8^{+} T cells from dissociated human tumors by FACS. Fold expression was calculated by dividing the MFI of PVRIG or TIGIT by the MFI of the IgG control. Grey line = No expression detected. Each orange dot is a distinct tumor sample and median of samples shown by the blue bar. C, D) Expression of PVRIG on CD8^{+} T cells vs PVRL2 on CD45^{-} cells or TIGIT on CD8^{+} T cells vs PVR on CD45^{-} cells is plotted from dissociated human tumors. Each dot represents an individual tumor sample.

PVRIG^{+}TIGIT^{+}PD1^{+} CELLS ARE THE HIGHEST % AND MOST EXHAUSTED OF CD8^{+} TILS

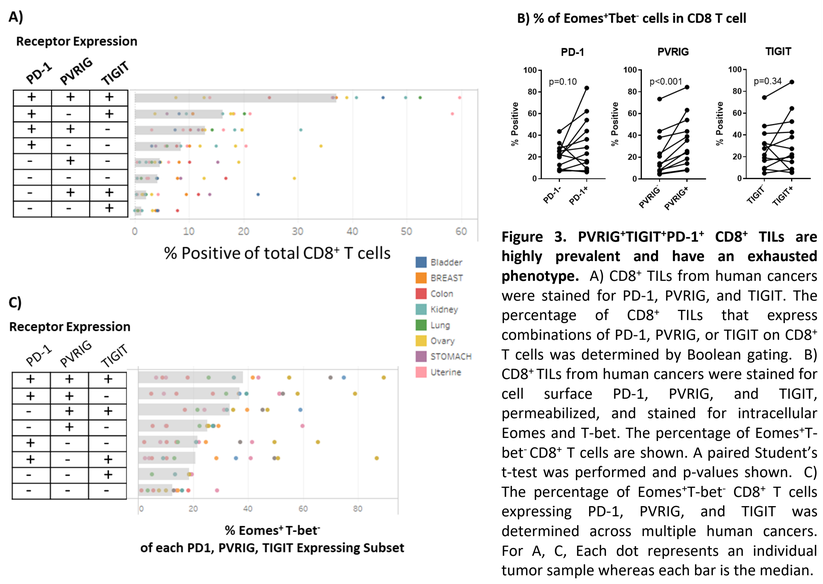

Figure 3. PVRIG^{+}TIGIT^{+}PD-1^{+} CD8^{+} TILs are highly prevalent and have an exhausted phenotype. A) CD8^{+} TILs from human cancers were stained for PD-1, PVRIG, and TIGIT. The percentage of CD8^{+} TILs that express combinations of PD-1, PVRIG, or TIGIT on CD8^{+} T cells was determined by Boolean gating. B) CD8^{+} TILs from human cancers were stained for cell surface PD-1, PVRIG, and TIGIT, permeabilized, and stained for intracellular Eomes and T-bet. The percentage of Eomes^{+}T-bet^{-} CD8^{+} T cells are shown. A paired Student's t-test was performed and p-values shown. C) The percentage of Eomes^{+}T-bet^{-} CD8^{+} T cells expressing PD-1, PVRIG, and TIGIT was determined across multiple human cancers. For A, C, Each dot represents an individual tumor sample whereas each bar is the median.

RELATIVE EXPRESSION OF PVRL2 VERSUS PVR VARIES BY TUMOR TYPE

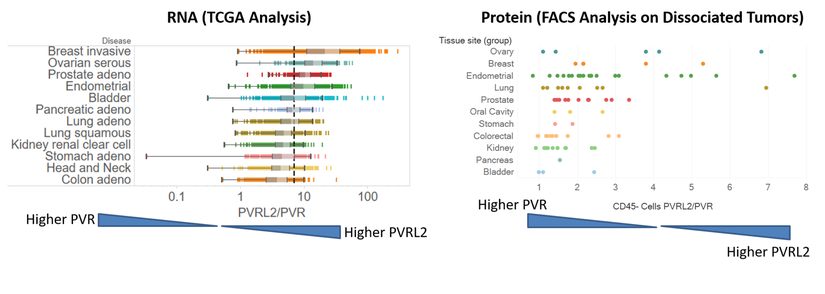

Figure 4. Relative RNA and protein expression of PVRL2 and PVR across different human tumors. RNA expression of PVRL2 and PVR from the TCGA was plotted as a ratio of PVRL2 relative to PVR across multiple human tumors (left hand panel). Tumors with higher PVRL2 RNA expression compared to PVR include breast, ovarian, prostate, endometrial, bladder, pancreatic and lung. The ratio of protein expression (gMFI) of PVRL2 relative to PVR on CD45^{-} tumor cells is plotted from dissociated human tumors (right hand panel). Each dot represents an individual tumor sample. Tumors with higher PVRL2 protein expression compared to PVR include ovary, breast, endometrial, lung, prostate, oral cavity and stomach. Higher RNA expression correlates with higher protein levels for PVRL2 across several tumors, including breast, ovarian, endometrial, prostate, and lung cancers.

PVRL2^{+}PVR^{-} TUMOR CELLS AND APCs EXIST IN HUMAN TUMORS

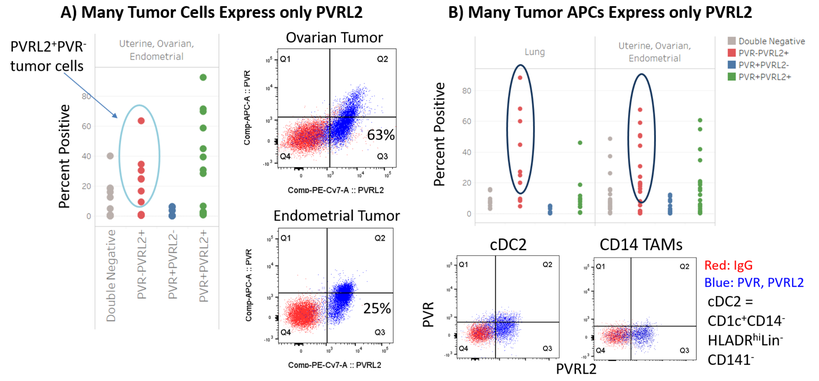

Figure 5. PVRL2^{+}PVR^{-} tumor cells and APCs are present in human tumors. PVRL2 and PVR expression from dissociated tumors determined by FACS on A) CD45- tumor cells, and B) cDC2 (CD1c^{+}CD14^{-}HLA-DR^{hi}Lin^{-}CD141^{-}) and CD14^{+} TAMs is plotted. PVRL2^{+}PVR^{-} tumor cells and APCs are represented as red dots in the percent positive plots. Representative FACS plots for PVRL2 and PVR expression (blue) as compared to an IgG isotype control (red) are shown for ovarian and endometrial tumors.

COM701 + COM902 COMBO HAS ACTIVITY ≥ PEMBROLIZUMAB ON PRIMARY CD3^{+} TILS

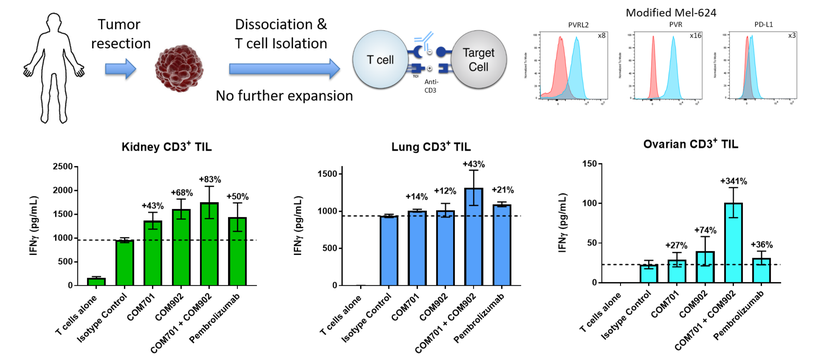

Figure 6: COM701 and/or COM902 have similar or greater potency than Pembrolizumab on freshly isolated human TILs. Human tumors obtained within 24 hours of surgical resection were dissociated and CD3^{+} TILs were purified. Isolated CD3^{+} TILs were co-cultured with a modified Mel-624 tumor cell line, expressing surface bound anti-CD3, and the indicated antibodies at 10 μg/ml. IFN-γ secretion in the conditioned media was measured at 72 hours. The percentage change in IFN-γ for each treatment over the hIgG isotype control is shown.

BLOCKADE OF PVRIG/PVRL2 INDUCES PD-1 AND TIGIT EXPRESSION

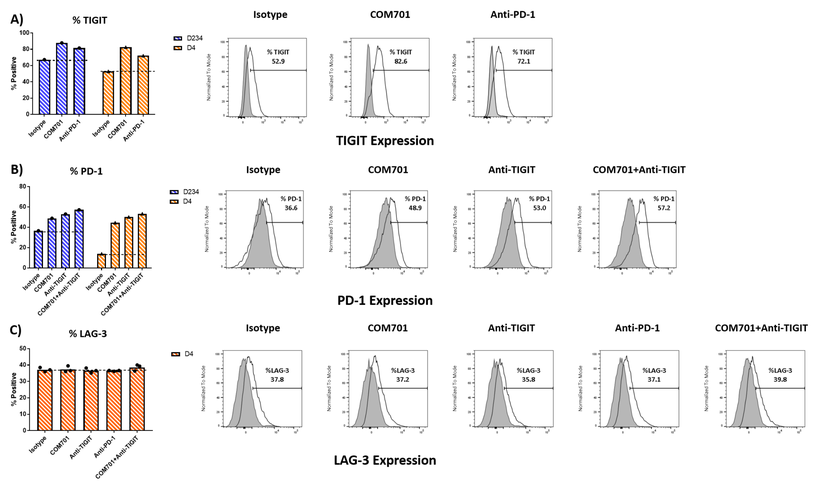

Figure 7: Blockade of PVRIG/PVRL2 induces PD-1 & TIGIT expression. CMVpp65-specific CD8^{+} T cells from 2 donors were co-cultured with Panc.05.04, CMVpp65 peptide, and the indicated antibodies at 10 μg/ml for 18 hrs. Cells were stained and the percentage of A) TIGIT^{+}, B) PD-1^{+}, and C) LAG3^{+} CD8^{+} T cells following each treatment is shown.

CONCLUSIONS

- PVRIG and TIGIT are non-redundant checkpoint receptors and promising targets for the treatment of cancer
- In tumors with higher PVRL2 than PVR, the PVRIG/PVRL2 interaction could be more dominant and require direct targeting of PVRIG